First principles calculation of chemical shifts in ELNES/NEXAFS of titanium oxides

1999 J. Phys.: Condens. Matter 11 3217

(http://iopscience.iop.org/0953-8984/11/16/003)

J. Phys.: Condens. Matter **11** (1999) 3217–3228. Printed in the UK PII: S0953-8984(99)00953-4

First principles calculation of chemical shifts in ELNES/NEXAFS of titanium oxides

Masato Yoshiya†, Isao Tanaka‡, Kenji Kaneko§ and Hirohiko Adachi†

† Department of Materials Science and Engineering, Kyoto University, Yoshida, Sakyo, Kyoto 606-8501, Japan
‡ Department of Energy Science and Technology, Kyoto University, Yoshida, Sakyo, Kyoto 606-8501, Japan
§ Ceramics Superplasticity Project, ICORP, JST, c/o JFCC, Atsuta, Nagoya 456-8587, Japan

Received 14 January 1999

Abstract. First principles molecular orbital calculations of three titanium oxides are made in order to quantify the absolute transition energies of ELNES/NEXAFS at the O K and Ti $L_{2,3}$ edges and to clarify the origin of their chemical shifts. The absolute transition energies as well as their chemical shifts at two edges are satisfactorily reproduced using clusters composed of 24 to 63 atoms when Slater's transition state method is employed allowing temporary spin-polarization. The O K edge shows a positive shift with the increase of the formal number of d electrons per Ti ion. The shift can be mainly ascribed to the variation of the energy of the t_{2g}-like band, although the energy of the O 1s core-orbital varies slightly. On the other hand, the Ti $L_{2,3}$ edge shows negative shift, which is found to be explained by the balance of energies of the Ti 2p and the t_{2g}-like band. The magnitude of the chemical shifts is not significantly altered by the manner of the octahedral linkage.

1. Introduction

With recent improvement of the field emission electronic gun (FEG), a convergent beam whose diameter is less than 1 nm is available. In combination with the transmission electron microscope (TEM), electron energy loss spectroscopy (EELS) offers various kinds of information within the atomistic region. Electron energy loss near edge structures (ELNES), which appears above the absorption edge in the EELS spectrum, has been attracting the interest of materials scientists for its capability as an analytical tool for electronic states of materials within the atomistic region. When the ELNES is measured in the transmission geometry, it is equivalent to NEXAFS (near edge x-ray absorption fine structure).

We can find two sorts of information in the experimental ELNES, although they are correlated to each other; one is the absolute energy of the absorption edge, which is recognized as the difference from that of reference materials, e.g., pure metal. The difference is referred to as 'chemical shift'. The other is the spectral shape composed of peaks. In order to obtain chemical/physical insight from the ELNES, theoretical calculation is essentially required. Several theoretical calculations are proposed to interpret the feature of the ELNES [1]. They are mainly divided into two categories. One is a multiple scattering (MS) calculation. The other is a first principles calculation on the basis of density functional theory (DFT). The MS calculations have been successful in reproducing the features of ELNES in many systems. The spectral shape in the experimental spectrum is interpreted with correlation between the energy position of the resonance peak above threshold and the distance between the excited

0953-8984/99/163217+12$19.50

atom and the backscattering cage [2]. Hence, it is rather difficult to obtain information on the chemical bonding states directly from the calculations. In addition, self-consistency of an excited electron is not achieved in the calculation. On the other hand, the DFT calculations provide information on the chemical bonding state together with the ELNES as unoccupied density of states (DOS). When all electrons are included in the calculation, accurate transition energy, which corresponds to the total energy difference between initial and final states, can be obtained.

Titanium oxide based materials are some of the most investigated materials for their importance in electronic or catalytic applications. Both experimental [3–5] and theoretical [6–9] studies have been extensively done. Brydson and coworkers have shown that major spectral features in the Ti $L_{2,3}$ edge and the O K edge ELNES originate from a slightly distorted octahedral unit of $[TiO_6]^{8-}$ [10]. They have performed the MS calculations to reproduce the spectral features found in the experimental spectrum. de Groot and coworkers have calculated O K edge NEXAFS by one of the DFT methods and concluded that the spectral difference between rutile and anatase in the higher energy region is ascribed to the smaller interaction of the Ti 4sp state in anatase due to the 8% less dense structure [11]. Tanaka and coworkers have applied ELNES to grain boundaries of polycrystalline $SrTiO_3$, where the ELNES obtained from grain boundaries exhibits a different spectral shape from that of the grain interior [12]. On the basis of understanding of chemical bonding states of rutile and $SrTiO_3$, they concluded that linkage of $[TiO_6]^{8-}$ in grain boundaries is different from that in $SrTiO_3$ grain interiors due to the removal of Sr^{2+} ions.

All the discussions shown above are focused only on the spectral shape by itself. However, the chemical shift provides further information on chemical bonding state. It should be a powerful analytical tool, especially when the structure or the chemical states of a material are unknown. Leapman and coworkers measured the chemical shift, in Ti-$L_{2,3}$ edge ELNES between Ti-metal and TiO_2(rutile) together with other sets of transition metal and metal oxides [13]. They compared the chemical shift in the ELNES with that in x-ray photoelectron spectroscopy (XPS). They concluded that the chemical shift in the ELNES and that in the XPS are not equivalent, since the physical phenomenon taking place during the energy loss process is different from that in the XPS. Soriano and coworkers have measured the Ti $L_{2,3}$ edge and O K edge NEXAFS of rutile before and after sputtering the sample by Ar ions, aiming at surface modification [14]. The chemical shift in the ELNES was discussed only by the analogy to the difference between pure metal and metal oxides. According to the measurements of XANES by Lusvardi and coworkers [15], the chemical shift is sensitive both in the Ti $L_{2,3}$ edge and in the O K edge among TiO_2 (rutile), Ti_2O_3 and TiO. They used the chemical shift for the fingerprinting procedure. However, no explanation from the viewpoint of chemical bonding states is given.

So far, despite the importance of the chemical shift in ELNES, quantitative theoretical calculations have not been done yet. That may be ascribed to the fact that calculation including core electrons is required for quantification of the chemical shift in ELNES. Although the energy loss process measures electronic excitation from a core orbital to an unoccupied orbital, most DFT calculations freeze the core orbitals for computational economy. In the present study, discrete variational (DV) $-$ Xα molecular orbital calculations [16, 17] have been performed for three titanium oxides, namely, TiO_2 (rutile), Ti_2O_3 and TiO, in order to explain the origin of chemical shifts in ELNES/NEXAFS together with spectral features. All core electrons are included in the calculations. Slater's transition state method [19] can therefore be applied for the evaluation of the absolute transition energy. In addition, effects of a core-hole can be rigorously computed by the molecular orbital calculations of model clusters that include a hole in a core orbital.

2. Computing procedures

The DV-Xα method is one of the molecular orbital (MO) methods based on the DFT. All the calculations in the present study have been performed using a computing code called SCAT [17]. The advantage of using the DV-Xα method in the present study is threefold.

(1) Numerical atomic orbitals (NAOs) are used as basis functions that are generated at each iteration by solving the radial part of the Schrödinger equation. Thus, the present NAO is sensitive to not only chemical environment but also temporary potential change due to the excitation of core electrons. The one-electron MOs are represented by linear combinations of NAOs, $\chi_i(r)$, i.e.,

$$\phi_l(r) = \sum_i C_{il}\chi_i(r). \tag{1}$$

In the present study, nearly minimal basis sets, namely, 1s–4p for Ti and 1s–2p for O, are used so that ELNES can be easily interpreted from the viewpoint of chemical bonding. The chemical bonding state is evaluated by the Mulliken population analysis [18]. Overlap population, Q_{ij}^l, in the lth MO and orbital population Q_i^l are obtained in the numerical integration manner by

$$Q_{ij}^l = C_{il}C_{jl}S_{ij} \tag{2}$$

$$Q_i^l = \sum_j Q_{ij}^l \tag{3}$$

where S_{ij} is the overlap integral. The net charge of the ion A, n_A, is obtained as

$$n_A = Z_A - \sum_l \sum_{i\in A} f_l Q_i^l \tag{4}$$

where f_l is the occupation number of electrons in the lth MO and Z_A is the atomic number. In addition, oscillator strength for the excitation from the ith core orbital to the lth MO is directly calculated with numerical wave functions of MOs by

$$I_{il} = \tfrac{2}{3}\Delta E|\langle l|r|i\rangle|^2 \tag{5}$$

where ΔE denotes the transition energy of the excitation. The PACS (photoabsorption cross section) is proportional to I_{il}.

(2) Since all electrons are included in the calculation, the effect of orbital relaxation, especially that of the core orbital, during the electron excitation process, can be taken into consideration. Slater's transition state method [19] is employed to evaluate the transition energy accurately. In the method a half electron in a core orbital is removed to fill an unoccupied orbital. More detail of the computational procedure is described elsewhere [17].

(3) Wave functions are localized in the vicinity of a core-excited atom in general. Molecular orbital calculations using a decent cluster size should be better for reproduction of the localized state than a band-structure calculation unless a large super-cell calculation is conducted [21, 22].

3. Results and discussion

3.1. Energy levels of isolated ions

Formal charges of Ti in TiO_2, Ti_2O_3 and TiO are generally taken to be 4+, 3+ and 2+, respectively, fixing the formal charge of O to be 2−. In other words, the number of electron in the Ti 3d orbital is formally 0, 1 and 2, respectively. It may therefore be easy to start with

the energy levels of isolated Ti ions to discuss the chemical shifts. Effects of Madelung fields as well as linkage of TiO_6 octahedra will then be discussed later.

The one electron Hamiltonian is given by

$$h(r) = -\tfrac{1}{2}\nabla^2 + V_{N-e}(r) + V_{e-e}(r) + V_{XC}[\rho(r)]. \tag{6}$$

Each term in the right-hand side of the equation denotes an operator for kinetic energy, nucleus–electron attractive energy, electron–electron repulsive energy and exchange–correlation energy, in turn. Atomic calculations were performed for isolated ions and the components of eigenvalues of Ti 2p and Ti 3d orbitals for Ti^{4+}, Ti^{3+} and Ti^{2+} are summarized in table 1. Regarding the Ti 2p core orbital, the kinetic energy and the nucleus attractive energy are almost independent of the formal charge. With the increase of d electrons, the electron repulsive energy increases, which causes a higher eigenvalue of Ti 2p. The eigenvalue of Ti 3d orbital also increases with rising the number of d electrons. However, each component changes differently from that of Ti 2p. The electron repulsive energy decreases, in contrast to Ti 2p. The kinetic energy also decreases, but the nucleus attractive energy significantly increases with the increase of the number of d electrons. As a result, the energy eigenvalue increases. The different responses to the formal charge can be understood by the change of spatial distribution of each orbital. Expectation values of r for Ti 2p and Ti 3d orbitals are summarized in table 2. As can be seen, the Ti 3d orbital expands notably with rising number of d electrons, while the Ti 2p core orbital remains unchanged. The expansion makes both the kinetic energy and the electron repulsive energy decrease. The absolute value of the nucleus attractive energy decreases at the same time.

Table 1. Eigenvalues and their components (eV) of Ti 2p and Ti 3d obtained by atomic calculations of isolated ions.

		Eigenvalue	Kinetic energy	Nucleus attraction	Electron repulsion	Exchange–correlation
Ti^{4+}	2p	−500.88	1074.21	−2654.16	1169.02	−89.95
	3d	52.27	153.05	−660.55	479.80	−24.56
Ti^{3+}	2p	−479.12	1074.45	−2654.41	1190.86	−90.02
	3d	34.56	133.93	−613.98	468.64	−23.15
Ti^{2+}	2p	−460.90	1074.84	−2654.87	1209.18	−90.06
	3d	−19.42	113.95	−560.14	448.01	−21.24

Table 2. Expectation values of r (Å) of wave functions obtained by atomic calculations of isolated ions.

	Ti^{4+}	Ti^{3+}	Ti^{2+}
2p	0.55	0.55	0.55
3d	2.14	2.36	2.67

In addition, it is found that eigenvalues of Ti 4s/4p orbitals increase with the increase of d electrons. However, energy separation between Ti 3d and Ti 4s/4p decreases with the increase of d electrons. Since the lowest unoccupied molecular orbitals (LUMOs) of the titanium oxides are mainly composed of Ti 3d, these orbitals do not seem to play an important role for the chemical shift in both the Ti $L_{2,3}$ edge and O K edge. However, they are reflected in the spectral shape. We will see that in the later section.

It is expected that the atomic orbitals are more localized in the solid state, as compared with isolated ions. In order to extract only the effect of the localization on the energy separation

between Ti 2p and Ti 3d, atomic calculations were conducted in addition by applying an external well potential. The potential is 1.4 Å in radius and −68.0 eV in depth; the potential was made to decrease by $1/r$ outside the well. The expectation values of r of Ti 3d orbitals decrease to 2.07, 2.20 and 2.33 Å for Ti^{4+}, Ti^{3+} and Ti^{2+}, respectively. This accompanies the decrease of the eigenvalues of the Ti 3d orbitals. At the same time, the eigenvalues of the Ti 2p core orbitals decrease due to the decrease of electron repulsive energy. However, the energy separations between two orbitals remain almost the same. Consequently, the localization of the orbital solely does not affect to the energy separation between the Ti 2p and the Ti 3d orbitals.

3.2. Distorted TiO_6 tetrahedron in Madelung fields

In order to understand the deviation of the electronic structure of titanium oxides from the isolated titanium ions, two major contribution should be taken into account: (1) the electrostatic field (Madelung field) as a result of arrays of ions, and (2) the Ti–O covalent bonding. Molecular orbital calculations are performed for model clusters composed of a Ti ion and six coordinating O ions that are embedded in the Madelung field generated by point charges put outside the cluster. Atomic positions in each cluster are taken from the corresponding crystals.

The energy level diagram is shown in figure 1, where the energy is aligned at the top of the O 2p band in order to compare results from different clusters easily. The major component of a set of levels located between −8 and 0 eV is O 2p. Above 4 eV, two sets of levels, whose major component is Ti 3d, are seen. Hereafter they will be referred to as the O 2p band and Ti 3d band, respectively. The set of levels at the lower energy of the Ti 3d band originates from a triply degenerated t_{2g} symmetry orbital and a set in the higher energy originates from a doubly degenerated e_g symmetry orbital under the octahedral (O_h) symmetry. Although the symmetry is lowered in the structure of Ti_2O_3 and TiO_2 (rutile), these classifications are still useful, because the splitting of levels in t_{2g} and e_g are small. Ti 4s/4p levels are found above 15 eV. As a result of covalent interaction, the Ti 3d band is no longer purely composed of Ti 3d orbitals; the O 2p component is present in the Ti 3d band. At the same time, a small contribution of Ti 3d orbitals is present in the O 2p band. The O 2p and Ti 3d orbitals interact in a bonding manner in the O 2p band, whereas it is antibonding in the Ti 3d band. With the increase of d electrons, the occupation number of the antibonding orbital increases. As a result, the covalent bond strength between O 2p and Ti 3d orbitals decreases with the decrease of the formal charge of the Ti ion. In addition, with the increase of d electrons, energy separation between the Ti 3d band and O 2p band becomes larger, which results in weaker MO interaction between Ti 3d and O 2p orbitals. As a matter of fact, the band-width of O 2p becomes smaller with the increase of d electrons. The band-width of the Ti 3d band, which corresponds to the so-called t_{2g}–e_g splitting, also becomes smaller. The net charges of Ti ions are +3.1, +2.4 and +1.7 for $[TiO_6]^{8-}$, $[TiO_6]^{9-}$ and $[TiO_6]^{10-}$, respectively. They are 78%, 80% and 85% of their formal charges, Ti^{4+}, Ti^{3+} and Ti^{2+}.

Absolute transition energy in the Ti $L_{2,3}$ edge ELNES/NEXAFS corresponds to the energy separation between the Ti 2p core orbital and the Ti 3d unoccupied orbital neglecting orbital relaxation associated with the excitation. Figure 2 shows the energy differences between the Ti 2p core orbital and the t_{2g}-like Ti 3d orbitals as a function of the formal number of d electrons. Results by the MO calculations are compared with those by calculations of single ions embedded in the Madelung field. As can be seen in the figure, the dependency of the energy separation obtained by the atomic calculations with the Madelung field upon the number of d electrons is almost the same as those obtained for isolated ions shown in table 1. The energy separation obtained by the MO calculation for octahedral unit shows smaller dependence on the

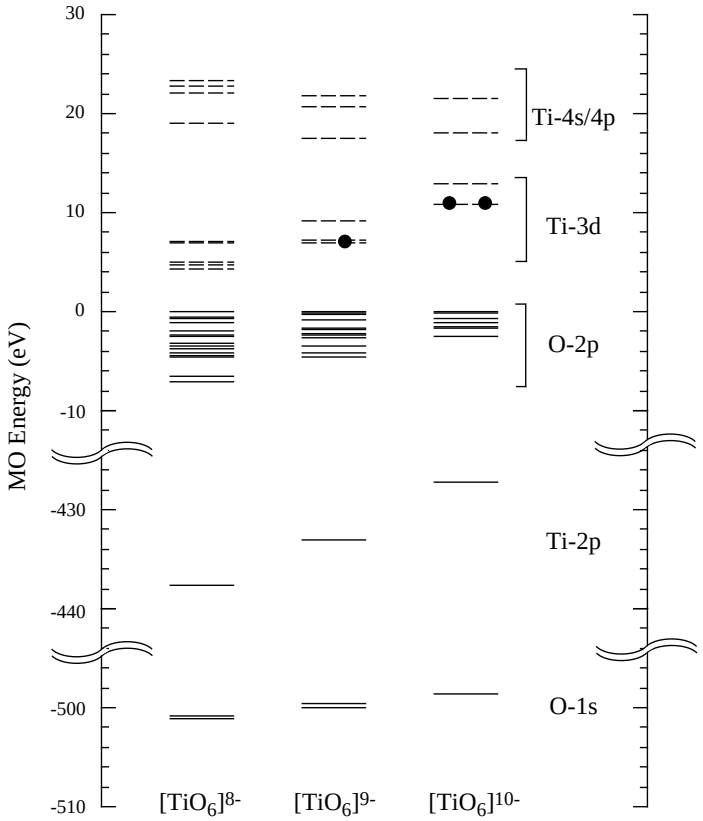

Figure 1. Energy level diagram obtained from calculations of three octahedral units. Energy is aligned at the top of the O 2p band. A solid line and a broken line denotes an occupied level an unoccupied/partially occupied level, respectively. A filled circle denotes an electron occupying the Ti 3d band.

number of d electrons. This can be explained by the magnitude of covalent bonding between Ti and O. As mentioned above, the Ti–O covalent bonding becomes stronger with the decrease of d electrons, leading to greater deviation from the energy separation of a single atom. These results suggest the positive chemical shift with the increase of the formal charge of Ti ion.

The chemical shift in the O K edge ELNES/NEXAFS is expected to be more complicated; the absolute transition energy of the O K edge corresponds to the energy separation between the O 1s core orbital and an unoccupied orbital where the major component is not the oxygen orbital but the Ti 3d orbital. The dependency of the O 1s core orbital and the t_{2g}-like Ti 3d orbital upon the number of d electrons can be seen in figure 1 and more precisely in figure 3.

One may suspect that energy of the O 1s core orbital is independent of the number of d electrons because the formal charges of the O ion remain $2-$. However the energies of the O 1s core orbital are found to increase with the increase of d electrons. This is due to the net ionicity of the O ion: with the increase of d electrons, the net ionicity of the O ion increases. In other words, more electrons are localized around O ions, which increases electronic repulsion, and hence its orbital energy. However, the dependency of the energies of the O 1s is smaller than that of the t_{2g}-like Ti 3d orbital. These results suggest negative chemical shift in the O K edge

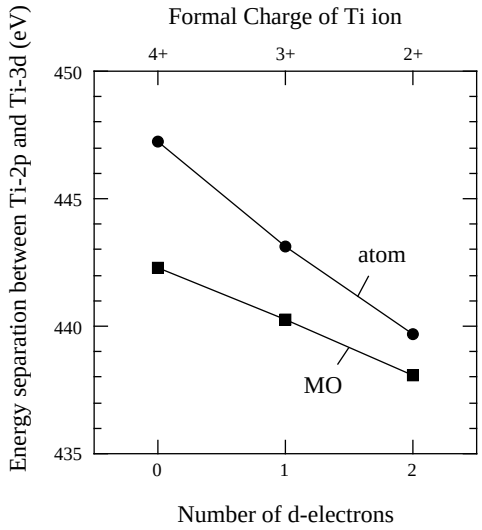

Figure 2. Energy separations between Ti 2p and Ti 3d obtained by atomic calculation with the Madelung field, and by the MO calculation for the $[TiO_6]^{n-}$ octahedral unit.

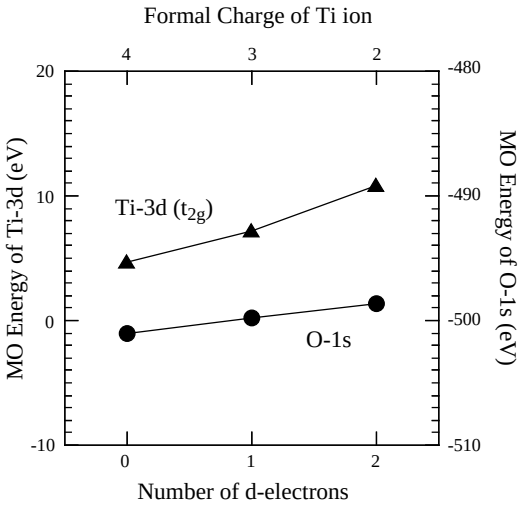

Figure 3. Dependency of the MO energy, which determines absolute transition energy at the O K edge, upon the number of d electrons.

with the increase of formal charge of Ti ion according to the Koopmans theorem neglecting orbital relaxation.

According to the results obtained for $[TiO_6]^{n-}$, a positive chemical shift in the Ti $L_{2,3}$ edge and a negative chemical shift in the O K edge are expected. Agreements of the obtained chemical shifts with the chemical shifts found in the experimental spectra are satisfactory. However, in order to evaluate the chemical shift more accurately, the effect of orbital relaxation associated with the electronic excitation and that of the octahedral linkage must be examined. These effects are evaluated in the next sections.

3.3. Evaluation of orbital relaxations

Due to an excitation of an electron from core orbital to an unoccupied orbital, the effective potential is altered, which accompanies orbital relaxation. Historically, the $Z+1$ approximation [20] is widely used for its simplicity, where the nuclear charge is increased by 1. However, the method is too rough; the method cannot tell the difference of potential changes, e.g., between that in the Ti K and the Ti $L_{2,3}$ edge.

In the present study, in order to obtain accurate transition energy, Slater's transition state method [19] is employed, where a half-filled electron is removed to fill an unoccupied orbital. Figure 4 shows the schematic energy level diagram of $[TiO_6]^{8-}$ for the ground state and two kinds of transition state. In the ground state (a), the energy of the O 1s core level is -501.0 eV. When a half-electron is removed from the O 1s orbital to fill the LUMO (b), the O 1s orbital goes down in energy to -531.2 eV. Hence the transition energy is 539.7 eV. However, the transition energy is overestimated, when the spin-polarization effect is neglected, even in the case of TiO_2 that shows no spin-polarization at the ground state. Accurate transition energy can be calculated only when temporary spin-polarization associated with the electronic excitation is taken into account as shown in figure 4(c). The transition energy in the ground state and those by the Slater transition state method with/without the temporary spin-polarization effects are compared in table 3. Calculations were made for a $[TiO_6]^{8-}$ cluster modelling the TiO_2(rutile). When the spin-polarization is allowed, the transition energy is 531.2 eV. The error of the transition energy is quite small. It is obvious that the accurate transition energy is obtained only when the effects of the orbital relaxation and of the spin-polarization are taken into account.

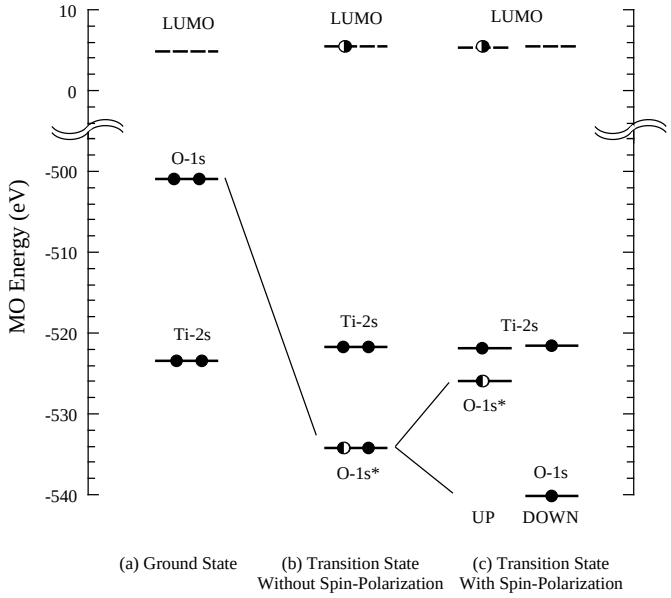

Figure 4. Schematic energy level diagrams obtained from a regular octahedral unit for TiO_2, (a) in the ground state, (b) in the transition state without the spin-polarization and (c) in the transition state with the spin-polarization. Only the O 1s core orbitals and the Ti 2s core orbitals are shown together with the lowest unoccupied molecular orbitals (LUMOs). A solid line and a broken line denotes an occupied orbital and an unoccupied orbital, respectively. A filled and a half-filled circle shows the occupation of an electron and a half-filled electron, respectively.

Table 3. Calculated transition energy (eV) obtained at the O K edge by the $[TiO_6]^{8-}$ model cluster for TiO_2 in comparison with the experiment [15]. Relative errors are shown in parentheses.

	Transition state		
Ground state	Without spin-polarization	With spin-polrization	Experiment
506.6	539.7 (+1.6%)	531.2 (−0.0%)	531.3

It may be interesting to note that the energy of a core-hole O 1s orbital is by accident very close to a Ti 2s orbital when the spin-polarization is allowed. Although this does not have any physical/chemical meaning, one had better carefully distinguish the two orbitals in the calculation.

3.4. Effect of octahedral linkage

With the results obtained from simple $[TiO_6]^{n-}$ clusters, the origin of the chemical shift is explained. The tendency of the chemical shift agrees with the experiment. In spite of the similar structural unit of TiO_6 octahedron, the manner of linkage of octahedra is different in each structure, keeping local charge neutrality. Except for vertex-sharing octahedra, an octahedral unit is connected to two octahedra with edge-sharing in TiO_2, one octahedron with face-sharing and three octahedra with edge-sharing in Ti_2O_3, and 12 octahedra with edge-sharing in TiO. In order to examine the modification by the different linkage of the octahedron in the real structure, calculations with larger model clusters cut from real structures have been performed for the Slater transition state allowing spin-polarization. In the present study, O-centred clusters of modest size, i.e., $[Ti_4O_{20}]^{24-}$, $[Ti_4O_{17}]^{22-}$ and $[Ti_6O_{19}]^{26-}$ are employed for TiO_2(rutile), Ti_2O_3, and TiO for calculations at the O K edge, respectively. For calculations at the Ti $L_{2,3}$ edge, Ti-centred model clusters, i.e., $[Ti_{11}O_{44}]^{44-}$, $[Ti_{14}O_{45}]^{79-}$ and $[Ti_{19}O_{44}]^{50-}$ are employed for TiO_2, Ti_2O_3 and TiO, respectively. For comparison with the experimental ELNES, PACS is obtained by calculating oscillator strength of the excitation from a core orbital to an unoccupied orbital. Discrete energies by the MO calculation are broadened by Lorenzian functions with 1.0 eV FWHM.

Calculated transition energies of the first distinct peak in the Ti $L_{2,3}$ edge and in the O K edge are summarized in table 4. Agreements between calculated transition energy and that in each experimental spectrum in the O K edge [15] are satisfactory. These are reproduced within 0.3% error of the experimental transition energies. The chemical shift in the O K edge in the theoretical spectrum is also well reproduced, although the shift in between TiO_2 and Ti_2O_3 and that in between Ti_2O_3 and TiO are slightly smaller and larger, respectively, than in the experimental spectra. Regarding the transition energy in the Ti $L_{2,3}$ edge, attention must be paid to the split of Ti $2p_{1/2}$ and Ti $2p_{3/2}$ due to the spin–orbit coupling. According to the atomic calculations for Ti^{4+}, Ti^{3+} and Ti^{2+} ions with and without taking relativistic effects into consideration, Ti $2p_{1/2}$ and Ti $2p_{3/2}$ orbitals are found to be smaller than the non-relativistic Ti 2p orbital by about 4.5 eV and greater than that by about 1.3 eV, respectively. By considering the energy differences in the atomic calculations, the calculated transition energies in the Ti L_3 and in the Ti L_2 edge are corrected, as shown also in table 4. Agreements of the experimental transition energies in the Ti L_3 edge with the corrected values are satisfactory. The chemical shift in the Ti L_3 edge is also reproduced well. It is hard to clearly distinguish the Ti L_2 edge spectrum from the experimental spectra due to the overlapping with the Ti L_3 edge spectrum. Although the manner of octahedral linkage is different in each structure, the tendency of the chemical shift found by $[TiO_6]^{n-}$ calculations are not significantly altered. The chemical shift

Table 4. Transition energies (eV) at the O K edge and at the Ti $L_{2,3}$ edge in comparison with the experimental values [15]. Calculated values for the Ti $L_{2,3}$ edge are corrected using the magnitude of Ti $2p_{1/2}$–Ti $2p_{3/2}$ splitting obtained by the relativistic atomic calculations.

		TiO_2	Ti_2O_3	TiO
O K	calc.	529.6	530.1	533.1
		(−0.3%)	(−0.4%)	(−0.0%)
	exp.	531.3	532.3	533.3
Ti $L_{2,3}$	calc. uncorrected	457.0	454.6	453.5
Ti L_2	calc. corrected	461.5	459.1	459.2
Ti L_3	calc. corrected	455.7	455.3	453.4
		(−0.7%)	(−0.8%)	(−0.6%)
Ti L_3	exp.	459.0	457.4	456.0

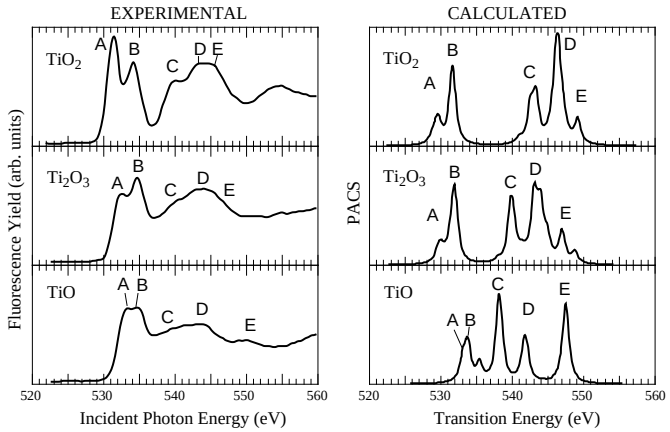

Figure 5. Calculated O K edge spectra for TiO_2, Ti_2O_3 and TiO, in comparison with the experimental spectra [15]. Peaks are assigned in the present study.

in O K edge is determined mainly by the variation of the energy of t_{2g}-like Ti 3d orbitals. On the other hand, that of the Ti $L_{2,3}$ edge is determined by the balance of energies of t_{2g}-like Ti 3d and Ti 2p orbitals.

Figure 5 shows calculated O K edge spectra for TiO_2(rutile), Ti_2O_3 and TiO, in comparison with the experimental O K edge ELNES [15]. Those of the Ti $L_{2,3}$ edge are compared in figure 6. Peaks originating from t_{2g}-like and e_g-like Ti 3d orbitals are labelled as A and B, respectively. Major peaks in the higher energy region that originate from Ti 4s/4p are labelled as C, D and E.

Regarding spectral shape in the O K edge ELNES, calculated spectra show qualitative agreement with the spectral features found in the experimental spectra. The major features found in the experimental spectra are threefold: (1) Splitting between A and B becomes smaller. (2) Ti 4s/4p band-width becomes larger. (3) The energy separation between the Ti 3d band and Ti 4s/4p band becomes smaller.

The splitting between A and B depends on the magnitude of covalent bonding as seen in section 3.2. As the number of d electrons increases, covalent bonding between Ti and O is weakened and energy separation between the Ti 3d band and O 2p band increases, which results in smaller band-width of Ti 3d. In contrast, the band-width of Ti 4s/4p becomes larger with

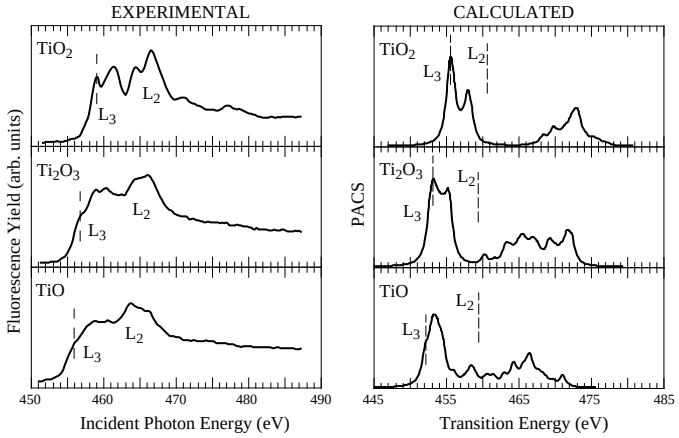

Figure 6. Calculated Ti L_3 edge spectra for TiO_2, Ti_2O_3 and TiO, in comparison with the experimental spectra [15]. Energies of calculated spectra are corrected.

the increase of d electrons. Although the contribution of Ti 4s/4p orbitals to chemical bonding is much smaller than the Ti 3d orbital, the contribution slightly increases as energy separation between the O 2p band and Ti 4s/4p band becomes closer, as shown in figure 1. In addition, the change of the manner of the octahedral linkage gives rise to direct Ti–Ti interaction. These two factors make the band-width of Ti 4s/4p wider with the increase of d electrons. The change of the separation between the Ti 3d band and Ti 4s/4p band originates from the energy separation found in the atomic calculations. According to the result, a negative chemical shift is expected in the Ti K edge with the increase of d electrons, since it measures the Ti 4p empty bands.

According to the dipole selection rule, the Ti 2p core electron is allowed to be excited into Ti 3d, Ti 4s (4d, 5s, 5d etc) unoccupied orbitals. Thus the spectral feature near the Ti $L_{2,3}$ edge mainly reflects Ti 3d and Ti 4s unoccupied states. In the Ti $L_{2,3}$ edge experimental spectra (figure 6), distinct peaks mainly composed of Ti 3d in the lower-energy region and small features mainly composed of Ti 4s in the higher-energy region are seen. Similar to the case of the O K edge, the splitting of the Ti 3d derived peaks becomes smaller and the width of the Ti 4s derived peaks becomes greater with the increase of d electrons. As a result, the experimental ELNES of TiO is rather featureless. The onset energy may be the only reliable information to characterize the states of Ti.

For further reproduction of the experimental spectra both in the Ti $L_{2,3}$ edge and in the O K edge, calculations by larger clusters with some extended basis functions may be required. It is, however, beyond the scope of the present study.

4. Concluding remarks

First principles molecular orbital calculations for three titanium oxides are performed in order to clarify the origin of the chemical shift. In ELNES, the absolute transition energy is determined by two orbitals. In the Ti $L_{2,3}$ edge, the chemical shift is determined by the balance of energies of Ti 2p and unoccupied t_{2g}-like Ti 3d. Since the energy of Ti 2p is more sensitive to the number of d electrons, the energy separation, which corresponds to the transition energy, is found to decrease with the increase of d electrons. In the O K edge, the chemical shift is determined by the balance of energies of the O 1s core orbital and the t_{2g}-like unoccupied Ti 3d. Although the energy of the O 1s core orbital is altered by the number of d electrons, the increase of the

energy of the t_{2g}-like Ti 3d affects more the transition energy, which results in larger transition energy with larger numbers of d electrons. By using larger sized model clusters, the tendency of the chemical shift is examined. Agreement of the transition energy with the experimental ELNES is satisfactory. It is also found that the tendency, obtained by the calculations with a octahedral unit, is not modified by introducing the effects of the linkage of the octahedra. The chemical shift found in both the Ti $L_{2,3}$ edge and in the O K edge are understood from the viewpoint of the chemical bonding state. The spectral shapes found in the experimental spectra in the Ti $L_{2,3}$ edge and in the O K edge are also reproduced by the present calculations and interpreted from the viewpoint of the chemical bonding state.

Acknowledgment

This work was supported by a Grant-in-Aid for General Scientific Research from the Ministry of Education, Sports, Science and Culture of Japan.

References

[1] Rez P, Bruley J, Brohan P, Payne M and Garvie L A J 1995 *Ultramicroscopy* **59** 159–67
[2] Bianconi A, Dell'Aricca M, Gargano A and Natoli C R 1983 *EXAFS and Near Edge Structure* ed A Bianconi, L Incoccia and S Stipcich (Berlin: Springer) p 57
[3] Fischer D W 1972 *Phys. Rev.* B **5** 4219–26
[4] Kurata H, Lefevre E, Colliex C and Brydson R 1993 *Phys. Rev.* B **47** 13 763–8
[5] Ruus R, Kikas A, Saar A, Ausmees A, Nommiste E, Aarik J, Uustare T and Martinson I 1997 *Solid State Commun.* **104** 199–203
[6] Grunes L A, Leapman R D, Wilker C N, Hofmann R and Kunz A B 1982 *Phys. Rev.* B **25** 7157–73
[7] Yamaguchi T, Shibuya S, Suga S and Shin S 1982 *J. Phys. C: Solid State Phys.* **15** 2641–50
[8] Nakai S, Mitsuishi T, Sugawara H, Maezawa H, Matsukawa T, Mitani S, Yamasaki K and Fujikawa T 1987 *Phys. Rev.* B **36** 9241–6
[9] de Groot F M F, Fuggle J C, Thole B T and Sawazky G A 1990 *Phys. Rev.* B **41** 928–37
[10] Brydson R, Sauer H, Engel W, Thomas J M, Zeitler E, Kosugi N and Kuroda H 1989 *J. Phys.: Condens. Matter* **1** 798–812
[11] de Groot F M F, Faber J, Michiels J J M, Czyzyk M T, Abbate M and Fuggle J C 1993 *Phys. Rev.* B **48** 2074–80
[12] Tanaka I, Nakajima T, Kawai J and Adachi H 1997 *Phil. Mag. Lett.* **75** 21–7
[13] Leapman R D, Grunes L A and Fejes P L 1982 *Phys. Rev.* B **26** 614–35
[14] Soriano L, Abbate M, Vogel J, Fuggle J C, Fernandez A, Gonzalez-Elipe A R, Sacchi M and Sanz J M 1993 *Surf. Sci.* **290** 427–35
[15] Lusvardi V S, Barteau M A, Chen J G, Eng J Jr, Fruhberger B and Teplyakov A 1998 *Surf. Sci.* **397** 237–50
[16] Ellis D E, Adachi H and Averill F W 1976 *Surf. Sci.* **58** 497–510
[17] Adachi H, Tsukada M and Satoko C 1978 *J. Phys. Soc. Japan* **45** 875–83
[18] Mulliken R S 1955 *J. Chem. Phys.* **23** 1833–40
[19] Slater J C 1974 *The Self-Consistent Field for Molecules and Solids (Quantum Theory of Molecules and Solids 4)* ed J L Farnsworth and C First (New York: McGraw-Hill)
[20] Fujikawa T 1983 *J. Phys. Soc. Japan* **52** 4001
[21] Tanaka I, Araki H, Yoshiya M, Mizoguchi T, Ogasawara K and Adachi H *Phys. Rev.* B submitted
[22] Mizoguchi T, Tanaka I, Yoshiya M, Oba F, Ogasawara K and Adachi H *Phys. Rev.* B submitted